



# Numerical modelling of relativistic shock acceleration

Athina Meli<sup>1,2</sup>

<sup>1</sup>Fundamental Interactions in Physics and Astrophysics, Department of Astrophysics, Geophysics and Oceanography  
University of Liege, Belgium

<sup>2</sup>Erlangen Center for Astroparticle Physics, Friedrich-Alexander-Universität Erlangen-Nürnberg, Germany

## Abstract.

The shock acceleration mechanism is invoked to explain non-thermal cosmic rays in Supernova Remnants, Active Galactic Nuclei and Gamma Ray Bursts jets. Especially, the importance of relativistic shock acceleration in extragalactic sources is a recurring theme raising a significant interest in the research community. We will briefly discuss the shock acceleration mechanism and we will address the properties of non-relativistic and relativistic shocks, particularly focusing on relativistic numerical Monte Carlo studies.

---

**Keywords.** Cosmic rays, shocks, acceleration, simulations

## 1 Outline

It is accepted that Super Novae Remnants (SNRs) are plausible environments for the acceleration of cosmic-ray particles up to energies of about  $10^{17}$ eV, while for the higher energies, Active Galactic Nuclei (AGN) and possibly Gamma Ray Bursts (GRBs) are favorable candidates. It is believed that the source of cosmic rays is plasma colliding at supersonic speeds, where shock waves form along with other instabilities, competing for the dissipation and acceleration mechanisms.

It is until now not fully understood to which extent the astrophysical bulk flows are due to leptonic flow (electrons and positrons) or baryonic flow (electrons and ions), and by which exact mechanisms this bulk flow energy can be converted into cosmic ray radiation, reaching energies of TeV and beyond. Evidence in form of power-law spectra of the observed cosmic ray radiation over wide energy intervals, favors the Fermi shock acceleration mechanism (i.e. first order Fermi acceleration), namely diffusive shock acceleration mechanism, which raises a significant interest in the research

---

*Correspondence to:* Athina Meli  
ameli@ulg.ac.be

community. In the diffusive shock acceleration mechanism particles experience a reflection by the local magnetic field and large-amplitude magneto-hydrodynamic waves on both sides of the shock. Particles can bounce back and forth across the shock, and via a shock velocity jump they increase their energy at each shock crossing (e.g. Bell 1978).

The fact that injected particles must be already relativistic is a requirement of the first order Fermi test particle approximation. This assumption requires the seed particles to have been already pre-accelerated. Pre-acceleration of particles is evident from observations in our solar system from e.g. sun coronal mass ejections to relativistic extragalactic sources such as AGN, GRBs and pulsars. The basic explanation for the essential presence of pre-accelerated seed particles in the regime of the acceleration, lies within scenarios of expanding plasma in an already pre-existed wind, or 'bubble' like features around the sites of acceleration.

Over the years we have been witnessing a plethora of techniques and methods of studying turbulent plasmas, shocks and particle acceleration at shocks. These methods are divided mainly into four main categories: i) the semi-analytic (simplified) method of solving the diffusion-convection equation (e.g. Eichler 1984) ii) the numerical method of solving the diffusion-convection equation allowing flow hydrodynamics and momentum dependent diffusion (e.g. Kang & Jones 2005) iii) the Monte Carlo simulation technique (e.g. Ellison & Double 2004, Meli et al. 2008) and finally iv) the Particle-in-cell method (e.g. Nishikawa et al. 2005, Dieckmann et al. 2009).

Generally, an analytical technique is effective in providing a close approximation to the diffusion-convection equation solution assuming that the particle distribution functions are almost isotropic. However, in many cases the observational data require numerical simulations for comparison. Especially in ultra-relativistic situations there is a clear need for numerical computations, as the particle anisotropy and large deviations in particle density, prevalent in highly relativistic

supersonic magnetized flows, do not allow an analytical solution. Especially, the problem of the scattering modes, plasma turbulence and distribution function of particles accelerated by highly relativistic collisionless astrophysical shocks, is currently under serious investigation by researchers using various means of calculation methods.

The pure numerical simulation techniques for describing collisionless plasmas are divided into two main types: the large scale techniques, and the smaller scale (Monte Carlo) ones.

In large scale plasma simulations, the trajectories of the particles are calculated from the magnetic and electric fields present in simulated plasma. These simulations account for most of our knowledge about collisionless shock structure and dissipation processes. This type of simulation approach can be divided into two main streams. Firstly, the simulations which self-consistently determine the electric and magnetic field from the particles, without requiring the use of predetermined assumptions of state equations and secondly, and those which follow particles in a predetermined electromagnetic environment (e.g. Steinolfson 1975, Shimada & Hoshino 2005).

In the smaller (Monte Carlo) scale method, a stochastic model is constructed in which the expectation value of a certain random variable (or more) is equivalent to the value of the physical quantity to be studied in the simulation. The value of the physical quantity to be defined is estimated by the average of several independent samples representing the random variable (Cashwell and Everett 1959). Naturally, a stochastic model adequate to the problem has to be assembled. Applying a Monte Carlo technique, means extensive use of a random number generation with the scope to simulate the random nature of a physical process. This aspect proves to be a powerful tool since large dynamic ranges in spatial and momentum scales are applied. In the Monte Carlo approach, the notion of test-particles is very efficient in describing particle random walks for a large number of particles.

In the following sections we will briefly discuss the shock acceleration mechanism, the limits of the maximum energies that cosmic rays can attain, the importance of relativistic shocks and their properties, briefly reviewing past findings, concluding with our results on relativistic shock acceleration Monte Carlo simulation studies.

## 2 Jets, shocks and particle acceleration

Shocks occur in supersonic plasma jets in which the injection plasma speed varies, namely in plasma flows which are surrounded by a medium of variable pressure. Specifically, the jets of AGN black holes are propelled by magnetic fields which are twisted by differential rotation of their central black hole accretion disk which fuels them, or by the

inertial frame dragging ergosphere (e.g. Blandford & Znajek 1977).

The magnetic field manifests through emitted radiation since it is frozen into the supersonic flowing jet plasma as it propagates outward from the central black hole. Observations indicate that AGN jets undergo a very large expansion at the exit from their inner black hole core. In a few parsecs its radius multiplies by more than a factor of a thousand. Due to the supersonic plasma velocities and disturbances in the pressure gradient, internal shock discontinuities form, where cosmic rays from the bulk plasma will eventually get accelerated through the first order Fermi acceleration mechanism as we will briefly describe further-on. For an extensive review see Jones & Ellison (1991).

Within an astrophysical jet, plasma elements consist of high relativistic populations of electrons and protons (plus positrons and nuclei) in order to assume a valid equation of state. It is interesting to note at this point that the physics of positively charged particles in jets is not yet very well known. The work of Wardle et al. (1998) supports the contribution of positrons. On the other hand, if one assumes that protons dominate, then little is known about their heat capacity ratio. Apart from the electron synchrotron emission, multiwavelength observations on the radiation continuum of AGN, favour many cases for proton acceleration at shocks emitting secondary radiation.

Furthermore, it is understood that the AGN jet emissions we observe, emerge from a plasma volume which is located very close to a shock formation, therefore originating from a thin layer of material downstream from the shock (see Dieckmann et al. 2009). The emitting material is optically thin and it is compressed on passing the shock structure downstream enhancing its emissivity.

Given shock formation(s) within a jet, cosmic particles are accelerated by stochastically crossing the shock discontinuity as they diffuse in the turbulent magnetic field, which is carried along with the plasma, upstream and downstream the shock. The average energy gain per shock cycle (e.g. Drury 1983) is given by

$$\frac{\Delta E}{E} = \frac{4}{3} \left( \frac{V_1}{c} - \frac{\cos\psi_2}{\cos\psi_1} \frac{V_2}{c} \right), \quad (1)$$

where  $V_1, V_2$  are the upstream and downstream plasma velocities in the shock rest frame respectively and,  $\psi_1, \psi_2$  indicate the inclination of the magnetic field vector to the shock normal, upstream and downstream.

The theory of first order Fermi acceleration mechanism by e.g. Axford (1977), Krymskii (1977), Bell (1978), etc shows that,

$$P(p) = \left( \frac{p}{p_o} \right)^{\frac{-3V_2}{V_1 - V_2}} \quad (2)$$

where  $P(p)$  represents the probability that a cosmic ray particle will cross a shock front enough times in order to

achieve a momentum  $p$  or higher. Then, the cosmic ray differential spectrum for 1D planar shocks will be given by

$$f(p) = \left(\frac{n_o}{p_o}\right) \left(\frac{3r}{r-1}\right) \left(\frac{p}{p_o}\right)^{-\left(\frac{2V_2+V_1}{V_1-V_2}\right)}, \quad (3)$$

where  $n_o$  is the upstream number density of particles per unit volume,  $p_o$  the initial momentum and  $r$  is the compression ratio,  $r = V_1/V_2$ , independent of the details of the diffusion. Thus, for a strong non-relativistic shock, i.e.  $r = 4$ , one obtains the differential particle spectrum as,  $f(p) \propto p^{-4} \propto E^{-2}$ . The remarkable point in the first order Fermi mechanism theory is that the calculated spectral index value of  $-2$ , is very close to the overall spectral index value of the differential cosmic ray spectrum observed on Earth. Of course it is understood that the remarkable feature of non-relativistic shock acceleration theory lies in the fact that the distribution of accelerated particles is scale-independent, i.e. a power-law, with a spectral index that depends only on the velocity compression ratio  $r$ . Nevertheless, as we will discuss later-on, this result does not carry over to *relativistic* shocks because of their strong plasma anisotropy. As a consequence, while power-laws are indeed created, the index becomes a function of the flow speed, the field obliquity, and the nature of the scattering, all of which closely control the degree of particle anisotropy.

Moreover, except of the standard value of  $r = 4$  for strong non-relativistic shocks, the choice of the canonical compression ratio  $r = 3$  is a well-known result for a relativistic purely hydrodynamic shock. However, one can envisage situations where the magnetic field becomes dynamically important. The classic example is the termination shock for the Crab pulsar wind, where Kennel & Coroniti (1984) observed that strong fields can weaken magnetohydrodynamic shocks considerably. Double et al. (2004) determined deviations from  $r = 3$  in highly relativistic shocks in the common cases where pressure anisotropy is significant. These deviations can either strengthen or weaken the shock, depending on the nature of the pressure anisotropy, which must be a significant function of the shock obliquity, i.e.  $\psi$ , thus in a relativistic shock one would anticipate the spectral index to be a function of  $\psi$ .

Before we move further, we stress out that non-relativistic shocks are well studied by now and their properties have been established as standard, functioning as a comparison basis for relativistic studies which will discuss later on. Two important points: (i) In non-relativistic shocks particles are everywhere in isotropy and the diffusive approximation solution of the transport equation can apply. (ii) The spectral index of the accelerated particles' power-law distribution is independent of inclination, scattering nature and strength of magnetic field.

### 3 Maximum cosmic ray energies

The Hillas (1984) condition poses the upper limit energy constraints for astrophysical objects, where it is assumed that

some kind of acceleration involving the magnetic field occurs: The maximum energy  $E_{max}$  that a charged particle (e.g. electron, proton, Fe nuclei) may acquire is proportional to the strength of the magnetic field of an astrophysical accelerator versus its size. This means that in principle the Larmor motion of the particle has to fit into the available space, independent of any other aspect. This aspect is given by the following equation

$$E_{max} \simeq Z \cdot e \cdot B \cdot V \cdot R \quad (4)$$

where  $Z$  is the atomic number,  $e$  the charge,  $B$  the magnetic field strength,  $V$  the velocity of the scattering centers,  $R$  the size of the acceleration site;  $R$  being larger than the Larmor radius of an energetic particle. We note that Hillas criterion is 'hidden' in the Lovelace limit (Lovelace 1976) Poynting flux condition

$$L_{jet} \simeq 10^{47} \text{erg/s} \left( \frac{E}{Z 10^{21} \text{eV}} \right)^2. \quad (5)$$

The Lovelace limit shows that the Poynting flux, a lower limit to the energy flux in an astrophysical jet, is connected to the maximal energy of a particle confined in the jet.

Moreover, since we assume diffusive shock acceleration in a shocked jet, based on the assumption of acceleration in a parallel shock, we assume  $V = V_{sh}$ , where  $V_{sh}$  denotes the velocity of the shock or in other words the upstream plasma flow ejecta. Later-on we will show that at relativistic shock conditions where  $V_{sh} \rightarrow c$ , the role of the inclination  $\psi$  of the magnetic field  $B$ , to the shock normal, in connection to the cosmic ray maximum energy  $E_{max}$  and spectral slopes, is of great importance (e.g. Meli & Quenby 2003, Baring 2004, Meli et al. 2008).

Jokipii's (1987) analytical work, and its numerical counterpart by Meli & Biermann (2006) showed that the maximum particle energy attained in a *non-relativistic* shock, is at its best in near-perpendicular shocks. Of course *ab initio* it should be assumed that the time scale for various losses such as bremsstrahlung or synchrotron is larger than the time scale needed for the acceleration process and secondly, the shock is a plane surface and not curved. Kobayakawa et al. (2002), based on Lagage and Cesarsky (1983), concluded into a single expression including the effect of the shock's inclination to the maximum attained energies as

$$E_{max} = Z e V_{sh} B R_{sh} \left( \frac{r-1}{rc\eta} \right) \cdot \left[ (\cos^2(\psi) + \frac{\sin^2(\psi)}{\eta^2}) + r(\cos^2(\psi) + r^2 \sin^2(\psi))^{-3/2} \cdot (\cos^2(\psi) + \frac{r^2 \sin^2(\psi)}{\eta^2}) \right]^{-1}$$

where here we assume  $\eta = \sqrt{1 + (\lambda/r_g)^2}$  which describes the field fluctuation component ( $\eta = 1$  corresponds to Bohm limit, i.e. strong scattering). One sees that for the limit of  $\psi = \pi/2$  (perpendicular shocks) one obtains  $E_{max} =$

$2ZeBR_{sh}\eta(V_{sh}/c)$ . An inspection of the last equation and equation (4) for parallel shocks, shows different qualitative approaches. Equation (4) is based on the concept of the size of the acceleration region, while the last equation considers the magnetic field inclination to the shock front and the fluctuation component which determine the actual acceleration rate of the process. Specifically, in the work of Meli & Biermann (2006) it was shown that the so called 'Jokipii limit',  $\eta$ , should be less than  $c/V_{sh}$  or in other words  $V_{sh}/c < \eta^{-1}$  for perpendicular non-relativistic shocks and, as higher the shock inclination as higher the maximum particle energy  $E_{max}$  attained (given  $\eta \gg 1$ ). At this point, one sees that equation (4) is actually recovered (essentially by a factor of 2 higher) in the limit of a non-relativistic perpendicular shock (i.e. perpendicular non-relativistic shocks are faster than parallel ones), since in the limit  $\eta = c/V_{sh}$  the term  $\eta V_{sh}/c$  equals 1 (see Meli & Biermann, 2010).

In general, in a shocked environment, flow into and out of the shock discontinuity is not along the shock normal (Begelman & Kirk 1990), but a transformation is possible into the so called normal shock frame (NSH) to render the flow along the normal. An important Lorentz transformation from the NSH frame, to the so called de Hoffmann-Teller frame (HT) (de Hoffmann & Teller 1950) can apply. In the HT frame the electric field  $\mathbf{E} = 0$ . Thus, one can study the diffusive shock acceleration mechanism in an 'electric-field-free' reference frame, boosting from the NSH frame by a speed  $V_{HT}$  along the shock surface as

$$V_{HT} \leq V_{NSH} \cdot \tan\psi. \quad (6)$$

Given relativistic shocks and by inspecting equation (6) it becomes obvious that then  $V_{NSH} \sim c$  and a HT transformation is allowed for all angles smaller than  $\tan\psi = 1$ , otherwise velocity  $V_{HT}$  will be greater than the speed of light. This physical causality gives rise to a classification of relativistic shocks into two categories. First, given  $V_{NSH} \sim c$ , one obtains the so called *subluminal* shock when its inclination is  $\tan\psi \leq 1$  (for these 'low-inclination' relativistic shocks the first order Fermi (diffusive) acceleration applies in the 'electric-field-free' HT frame). On the other hand, one obtains a *superluminal* shock when its inclination is  $\tan\psi > 1$  (in superluminal shocks particles are accelerated by the so called shock-drift acceleration mechanism in the presence of the electric field, see Armstrong & Decker, 1979. Considering a (near) perpendicular shock, a model involving shock-drift is the most appropriate).

#### 4 Monte Carlo numerical approach

In this paper we will present a simulation study based on a sophisticated relativistic test-particle Monte Carlo code, developed initially by Meli & Quenby (2003b) and extended by Meli et al. (2008). In the field of particle shock acceleration, since one assumes a diffusive turbulent plasma media, the

Monte Carlo technique actually gives a solution to the time independent Boltzmann equation

$$\Gamma(V + v\mu) \frac{\partial f}{\partial x} = \frac{\partial f}{\partial t} \Big|_c, \quad (7)$$

where a steady state is assumed in the shock rest frame,  $V$  is the fluid velocity,  $v$  the velocity of the particle,  $\Gamma$  is the Lorentz factor of the fluid frame,  $\mu = \cos\theta$  the cosine of the particle's pitch angle  $\theta$  and  $\partial f/\partial t|_c$  is the collision operator.

The first order Fermi (diffusive) acceleration is then simulated provided there is a shock front, where the particles' guidance-centre undergoes consecutive scatterings with the assumed magnetized media. In each shock crossing particles gain an amount of energy prescribed by the appropriate jump condition equations. In principle, the basic coordinate system to describe a shock is a Cartesian system  $xyz$ , where the shock plane lies on the  $yz$  plane. We define the shock at  $x = 0$ , while  $x < 0$  corresponds to the upstream region and  $x > 0$  to the downstream one. The direction of the flow in the shock rest frame is in the positive direction that is, from upstream to downstream. The reference frames used during the simulations are the upstream and downstream fluid rest frames, the NSH frame and the HT frame. The particles have an initial boost of  $\gamma \sim (\Gamma_{sh} + 10)$  as they are injected upstream towards the shock and they are allowed to scatter in the respective fluid rest frames with their basic motion described by a guiding centre approximation.

While in the subluminal case, particle transmission at the shock can be decided in the HT frame employing conservation of the first adiabatic invariant (Hudson 1965), in the superluminal case computations are followed entirely in the fluid rest frames with reference to the NSH frame, simply employed to check whether upstream or downstream shock conditions apply. Thus, superluminal shock acceleration is treated as a shock drift acceleration mechanism in the NSH frame, and it is best viewed when the shock is nearly perpendicular (Meli & Quenby 2003b).

Begelman & Kirk (1990) pointed out, that in the blast wave frame of an astrophysical jet the turbulence can be isotropic and many shock stationary frame configurations can be superluminal. Nevertheless, many polarization observations, show that chaotic magnetic fields prevail at distances larger than a few parsecs, but there should be statistically anisotropic to produce a net linear polarisation as discussed in Korchakov and Syrovatskii (1962). To this end, Laing (1980) has pointed out that a chaotic magnetic field being initially isotropic becomes anisotropic after crossing a shock front due to the plasma compression. Moreover, Meli & Quenby (2003b) showed that a transformation from an initially isotropic rest frame distribution to an accelerated flow frame, leads to a comoving relativistic plasma frame field distribution, lying close to the flow vector. This condition allows for a range of subluminal situations when viewed in the shock rest frame.

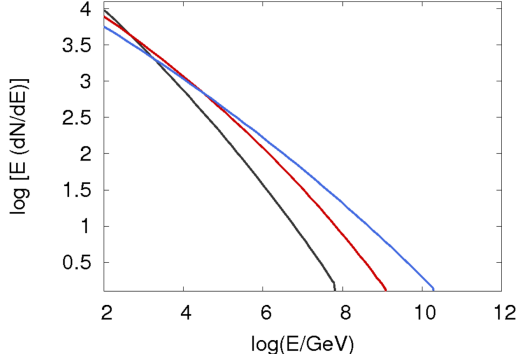


**Fig. 1.** An exemplary graph showing differential particle spectra for a shock inclination of 45 degrees, scattering of  $< \pi/4$  and three different shock Lorentz factors of 5, 20, 50 (respectively from lower to upper graph).

$\Gamma$	$\sigma(\psi = 45^\circ, \theta \leq \pi)$	$\sigma(\psi = 0^\circ, \theta \leq \pi)$	$E_{max}[eV]$
5	2.17	2.03	$\sim 10^{17.5}$
20	2.05	1.96	$\sim 10^{18}$
50	2.00	1.90	$\sim 10^{19}$

**Table 1.** *Subluminal* mild relativistic shocks: spectral indices ( $\sigma$ ) for different shock Lorentz factors ( $\Gamma$ ), two inclination angles ( $\psi$ ), a large-angle scattering ( $\theta \leq \pi$ ) and maximum attained energies  $E_{max}$ .

Particle scattering by magnetic irregularities fixed in the plasma rest frame is assumed and as discussed in Meli et al. (2008) it is justified in neglecting fluid frame acceleration beyond the region of trajectory intersection with the shock surface. The scattering operator is treated via large angle diffusion or a pitch angle scattering approach. Standard theory poses the conservation of the first adiabatic invariant in the HT frame in order to determine reflection or transmission of the particles. Reflection of particles during diffusive acceleration is important in oblique shocks since it contributes to the overall efficiency of acceleration. In the HT frame the allowed and forbidden angles for transmission depend only on the input pitch and phase, not on rigidity, thus the results of Hudson (1965) apply in our model. In the relativistic shock situation anisotropy renders the input to the shock from upstream very anisotropic in pitch angle, but as was discussed in Meli (2003), it is an acceptable approximation to randomise phase before transforming to the HT frame and then to use the adiabatic invariant to decide on reflection/transmission, based on Hudson's (1965) results. For further details on the Monte Carlo numerics and particle kinematics the reader is referred to Meli & Quenby (2003a,b) and Meli et al. (2008) and references there in.

$\Gamma$	$\sigma(\psi = 45^\circ, \theta \leq \pi/4)$	$\sigma(\psi = 0^\circ, \theta \leq \pi/4)$	$E_{max}[eV]$
5	2.25	2.19	$\sim 10^{17}$
20	2.12	2.11	$\sim 10^{18}$
50	2.10	2.08	$\sim 10^{19}$

**Table 2.** *Subluminal* mild relativistic shocks: spectral indices ( $\sigma$ ) for different shock Lorentz factors ( $\Gamma$ ), two inclination angles ( $\psi$ ), a chosen pitch angle diffusion ( $\theta \leq \pi/4$ ) and maximum attained energies  $E_{max}$ .

$\Gamma$	$\sigma(\psi = 45^\circ, \theta \leq 10/\Gamma)$	$\sigma(\psi = 0^\circ, \theta \leq 10/\Gamma)$	$E_{max}[eV]$
100	1.91	1.83	$\sim 10^{19}$
300	1.86	1.76	$\sim 10^{20}$
900	1.52	1.41	$\sim 10^{20.5}$

**Table 3.** *Subluminal* high relativistic shocks: spectral indices ( $\sigma$ ) for different shock Lorentz factors ( $\Gamma$ ), two inclination angles ( $\psi$ ) with a very small pitch angle diffusion angle ( $\theta \leq 10/\Gamma$ ) and maximum attained energies  $E_{max}$ .

## 5 Relativistic shocks

Considerable work has been conducted over the last decades regarding particle shock acceleration especially, by relativistic shocks, bound mostly to numerical approximations and simulation techniques. Early work on relativistic shocks was mostly analytic in the test-particle approximation, where the accelerated particles did not contribute significantly to the global hydrodynamic structure of the shock, see e.g., Peacock (1981), Kirk & Schneider (1987), Heavens & Drury (1988). As aforementioned, the important aspect that distinguishes relativistic shocks from non-relativistic ones lies in the inherent anisotropy due to rapid convection of particles through and away downstream of the shock, which renders analytic approaches more difficult. Assuming relativistic shocks, semi-analytical approaches were possible for the limit of extremely small angle scattering, namely pitch-angle diffusion, by authors such as, e.g., Kirk & Schneider (1987) etc. On the other hand, complementary Monte Carlo techniques have been employed for relativistic shocks by a number of authors, including test-particle approximations for steady state shocks of parallel and oblique magnetic fields, see e.g. Ellison et al. (1990), Ostrowski (1991), Meli & Quenby (2003a,b), Ellison & Double (2004), etc. In principal all these studies show the trend of cosmic ray spectral

$\Gamma$	$\sigma(\psi = 85^\circ, \theta \leq 10/\Gamma)$	$\sigma(\psi = 65^\circ, \theta \leq 10/\Gamma)$	$E_{max}[eV]$
100	2.48	2.33	$\sim 10^{15}$
300	2.35	2.28	$\sim 10^{15.5}$
900	2.21	2.19	$\sim 10^{16}$

**Table 4.** *Superluminal* high relativistic shocks: spectral indices ( $\sigma$ ) for different shock Lorentz factors ( $\Gamma$ ), two inclination angles ( $\psi$ ), a small pitch angle diffusion angle ( $\theta \leq 10/\Gamma$ ) and maximum attained energies  $E_{max}$ .

index flattening as a function of shock velocity.

Moreover, it is accepted by now that when relativistic shocks are involved in particle acceleration, it seems that the slope of the non-thermal distribution is dependent on the nature of scattering, except the dependence on shock inclination, that is on the magnetic field configurations, a feature evident in the work of e.g. Bednarz & Ostrowski (1998). It is interesting also to note that the so called large-angle scattering yields kinematically structured and flatter distributions for relativistic shocks, see e.g. Ellison et al. (1990), Meli & Quenby (2003b), Baring (2004).

There used to be a general belief that a 'universal' power-law index of  $-2.2$  must be obeyed by both non-relativistic and relativistic shocks, see Achterberg et al. (2001). Nevertheless, it is important to clarify at this point, that such a claim applies only for *parallel* relativistic shocks and for extremely small pitch angle (or fine) scattering. Fine scattering denotes the number of particle scatterings after a fraction of a gyroperiod within a maximum angle  $\delta\theta_{max} = \sqrt{(6\delta t/t_c)}$ , where  $\delta t$  is the time between pitch-angle scatterings and  $t_c = \lambda/v$ ;  $v$  particle's velocity and  $\lambda$  its mean-free-path.  $\lambda$  is proportional to the gyroradius  $r_g = pc/(eB)$  ( $e$  is the electronic charge and  $B$  is the local uniform magnetic field in Gaussian units), i.e.,  $\lambda = \xi_{mfp} r_g$ , where  $\xi_{mfp}$  is a measure of the *strength* of scattering. In the Bohm diffusion (strong scattering limit) one has  $\xi_{mfp} = 1$ . Furthermore, setting  $\delta t = \tau_f/M_f$ , where  $M_f$  much greater than 1 denotes the number of gyro-time segments  $\delta t$ . Dividing a gyro-period  $\tau_f = 2\pi r_g/v$ , one obtains  $\delta\theta_{max} = \sqrt{(12\pi/(\xi_{mfp} M_f))}$ , and the scattering properties of the medium can be modeled with the two parameters  $\xi_{mfp}$  and  $M_f$ .

Since the turbulence in a shocked media can vary significantly, one cannot exclude a possible variety of collision and diffusion operators in different astrophysical environments (Quenby & Meli, 2005). Thus, this asymptotic claimed 'universal' index of  $-2.2$  refers to the case of the mathematical limit of extremely small pitch angle diffusion, where the particle momentum is stochastically deflected on arbitrarily small angular (and therefore temporal) scales. Such a pitch angle scattering results when the scattering angle  $\theta$  is taken to be inferior to the Lorentz cone angle  $1/\Gamma_{up}$  ( $\Gamma$  the Lorentz factor) in the upstream region. In this case, particles diffuse in the region upstream of a *parallel* shock only until their angle to the shock normal exceeds around  $1/\Gamma_{up}$ . Then they are rapidly swept to the downstream side of the shock. To this end, numerical calculations of relativistic shock acceleration by e.g. Meli & Quenby (2003b), Ellison & Double (2004), Stecker et al. (2007), Meli et al. (2008), etc, have shown a clear deviation of the spectral index value connected to shock inclination or different scattering types.

Here, we conduct a numerical study for relativistic particle shock acceleration based on the Monte Carlo code described in section 2, with the aim to overview the properties of relativistic shocks, straightforwardly drawing the attention on the importance of their inclination [i.e. low-inclined (sub-

luminal) or highly-inclined (superluminal) shocks] and scattering type in connection to spectral slopes and maximum attained energies. We calculate a differential particle spectrum fitting a power law given by,  $dN/dE \propto E^\sigma$ , where  $dN$  is the number of particles with energies in the interval  $E$  to  $E + dE$ ,  $\sigma$  being the spectral index. Since our simulation method is of the test-particle approach we normalize the energies assuming protons as the primary particle population of acceleration. The simulations results, see Tables 1-4, are summarized as follows:

- 1) Mild relativistic ( $5 \leq \Gamma \leq 50$ ) subluminal parallel shocks ( $\psi = 0^\circ$ ) with a *large angle scattering* type of  $\theta \leq \pi$ , generate slightly flatter particle spectra than the oblique shocks ( $\psi = 45^\circ$ ), see table 1.
- 2) Mild relativistic ( $5 \leq \Gamma \leq 50$ ) subluminal parallel shocks ( $\psi = 0^\circ$ ) with a *pitch angle diffusion* type of  $\theta \leq \pi$ , produce as well slightly flatter particle spectra than the oblique shocks ( $\psi = 45^\circ$ ), see table 2. In general, a scatter of pitch angle diffusion generates slightly steeper spectra compared to the the large angle scattering type.
- 3) Highly relativistic ( $100 \leq \Gamma \leq 900$ ) subluminal parallel shocks ( $\psi = 0^\circ$ ) with a very small pitch angle diffusion type of  $\theta \leq 10/\Gamma$ , produce as well slightly flatter particle spectra than the oblique shocks ( $\psi = 45^\circ$ ), see table 3. Nevertheless all spectral indices for the highly relativistic shock cases are flatter than the mild relativistic ones, confirming past findings of various authors regarding the flatness of particle spectra as a function of highly relativistic flows. Finally,
- 4) highly relativistic ( $100 \leq \Gamma \leq 900$ ) *superluminal* shocks with exemplary inclinations of  $\psi = 65^\circ$  and  $\psi = 85^\circ$  and a very small pitch angle diffusion scatter of  $\theta \leq 10/\Gamma$  generate the steepest spectra compared to all subluminal cases described above. Moreover, from the numbers in Tables 1-4 and figure 1, on sees that subluminal shocks are very efficient accelerators comparing to the superluminal cases.

## 6 Summary

The shock acceleration in Supernova Remnants, AGN and GRBs jets can explain the non-thermal origin of the cosmic rays. Relativistic particle shock acceleration is an important mechanism which is claimed to account for the highest cosmic ray energies as well as the variety of irregular primary spectra originating from such sources.

Considerable work has been conducted over the last decades regarding particle acceleration by relativistic shocks, via numerical approximations and simulation techniques. A vital characteristic that distinguishes relativistic shocks from its non-relativistic counterparts is the inherent anisotropy due to rapid convection of particles through and away downstream of the shock, which renders difficulties in analytic approximations. Complementary Monte Carlo techniques have been developed over the years for studying relativistic shocks, which successfully proven to be very efficient accelerators. Numerical studies by different authors on relativistic

shock acceleration indicate a clear deviation of the spectral index value connected to shock speed, scattering type or the inclination of the shock to the magnetic field. These facts rendering important implications to consequent gamma-ray and neutrino emission models originating from extragalactic relativistic sources.

*Acknowledgements.* With special thanks to collaborators J. Quenby, P. L. Biermann and J. K. Becker. The author would like to thank the two anonymous referees for valuable corrections and suggestions, and she acknowledges the ECRS committee for the invitation to present this work.

## References

- Achterberg, A. Gallant, Y. A., Kirk, J. G., Guthmann, A., 2001, *MNRAS*, 328, 393
- Armstrong, T. P., Decker, R. B., 1979, 'Particle acceleration mechanisms in astrophysics', AIP proc, no 55, p101
- Axford, W. I., 1977, ICRC Conf. Proc., 11, 132
- Baring M., 2004, *Nucl.Phys.*, 136, 198
- Bednarz, J., Ostrowski, M., 1996, *MNRAS*, 283, 447-456
- Bell A. R., 1978, *MNRAS*, 182, 147
- Begelman, M. C., Kirk, J. G., 1990, *ApJ*, 353, 66
- Blandford R. D., Znajek R. L., 1977, *MNRAS*, 179, 433
- Cashwell E. D., Everett, C., J., 1959, 'Monte Carlo Method for random walk problems', Pergamon Press de Hoffmann, F., Teller, E., 1950, *Phys. Rev.* 80, 692
- Dieckmann M. E., Murphy G., Meli A., Drury L. O' C., 2010 *A&A*, 509A, 89
- Double, G., Baring, M., Jones, D. Ellison, D. 2004, *ApJ*, 600, 485
- Drury, L O', 1983, *RPPh*, 46, 973
- Heavens, A. F., Drury, L.O'C., 1988, *MNRAS* 235, 997
- Hillas A. M., 1984, *ARA&A*, 22, 425
- Hudson, P. D., 1965, *MNRAS* 131, 23
- Jones, T. W., Kang, H., 2005, *ApJ*, 24, 75
- Jones, T. W. and Ellison, D. C., 1991, *SSRv*, 58, 259
- Jokipii, J. R., 1987, *ApJ*, 313, 842
- Ellison, D. C., Reynolds, S. P., Jones, F. C., 1990, *ApJ*, 360, 702
- Ellison, D. C., Double, G. P., 2004, *ApPh* 22, 323
- Eichler, D., 1984, *ApJ*, 277, 429
- Kennel, C. F., Coroniti, F. V. 1984, *ApJ*, 283, 694
- Kirk, J. G., Schneider, P., 1987, *ApJ*, 322, 256
- Kobayakawa K., Honda Y. S., Samura T., 2002, *PhRvD*, 66h, 3004
- Korchakov, A. A., Syrovatskii, S. I., 1962 *SvA*, 5, 678
- Krymskii G. F., 1977, *Akademiia Nauk SSSR Doklady*, 234, 1306
- Laing, R. A., 1980, *MNRAS*, 193, 439
- Lagage P. O. & Cesarsky C. J., 1983, *A&A*, 125, 249
- Lovelace, R. V. E., 1976, *Nature*, 262, 649
- Meli, A., 2003, Ph.D. Thesis, Imperial College of Science, Technology and Medicine, London, UK
- Meli A. & Quenby J. J., 2003, *ApPh*, 19, 637
- Meli A. & Quenby J. J., 2003, *ApPh*, 19, 649
- Meli A. & Biermann P. L., 2006, *A&A*, 454, 687
- Meli A., Becker J. K., Quenby, J. J., 2008, *A&A*, 492, 323
- Meli A. & Biermann P. L., 2010, submitted in *A&A*
- Nishikawa, K.-I., Ramirez-Ruiz, E., Hardee, P., Hededal, C., Kouveliotou, C., Fishman, G. J., Mizuno, Y., 2005, *AAS*, 207, 7503
- Ostrowski, M., 1991, *MNRAS*, 249, 551
- Peacock, J. A., 1981, *MNRAS* 196, 135
- Quenby, J. J., Meli, A. 2005, *Geophysical Monograph*, 156, AGU, Washington, DC, 9
- Shimada N., Hoshino M., 2000, *ApJ*, 543I, 67
- Stecker F. W., Baring J., Summerlin E. J., 2007, *ApJ*, 667L, 29
- Steinolfson et al. 1974, 'Solar Wind 3, Third Conference', proc. p 175.
- Wardle J. F. C., Homan D. C., Ojha R., Roberts D. H., 1988, *Nature*, 395, 457